On Active Surge Control of Compression Systems via Characteristic Linearization and Model Nonlinearity Cancellation

Yohannes S.M. Simamora[1,3], Harijono A. Tjokronegoro[1,2] & Edi Leksono[2]

[1]Instrumentation and Control Graduate Program, Institut Teknologi Bandung
[2]Engineering Physics Research Group, Institut Teknologi Bandung
Jalan Ganesha 10, Bandung 40132, Indonesia
[3]Mechanical Engineering Study Program, Politeknik Purbaya
Jalan Pancakarya 1, Talang, Kabupaten Tegal 52193, Indonesia
Email: simamora@me.purbaya.ac.id

Abstract. A simple approach of active surge control to compression systems is presented. Specifically, nonlinear components of the pressure ratio and rotating speed states of the Moore-Greitzer model are transferred into the input vectors. Subsequently, the compressor characteristic is linearized into two modes, which describe the stable region and the unstable region respectively. As a result, the system's state and input matrices both appear linear, to which linear realization and analysis are applicable. A linear quadratic regulator plus integrator is then chosen as closed-loop controller. By simulation it was shown that the modified model and characteristics can describe surge behavior, while the closed-loop controller can stabilize the system in the unstable operating region. The last-mentioned was achieved when massflow was 5.38 per cent less than the surge point.

Keywords: *active surge control; compression systems; linear quadratic regulator; nonlinear model; nonlinearity cancellation.*

1 Introduction

The characteristic and operating area of a compressor can be described by a compressor map as shown in Figure 1. The characteristic is a function of nondimensional pressure ratio (ψ) against nondimensional mass flow (ϕ), as shown in Figure 1. A surge line divides the compressor operating area into a stable region and a surge/unstable region. When compression takes place, massflow is reduced so that it moves toward the unstable region. If mass flow is left to pass through the surge line, the compressor will enter its unstable operating region and undergoes surge.

Surge is a compressor instability phenomenon when pressure ratio and massflow fluctuate with a large amplitude. The fluctuations result in a limit cycle in the compressor map. Since it reduces efficiency and may even damage

Received September 19th, 2012, Revised February 7th, 2014, Accepted for publication May 20th, 2014.
 ISSN: 2337-5779, DOI: 10.5614/j.eng.technol.sci.2014.46.3.8

the compressor, the presence of surge is highly undesired in any compressor operation.

The traditional and most-used approach in dealing with surge is surge avoidance. While its implementation strategies may vary, the basic idea of surge avoidance is simply to prevent the compressor from entering the unstable operating region. This can be achieved by defining a surge margin close to the surge line in the stable region, as shown in Figure 1. However, this approach has an inherent drawback, i.e. the limitation of the compressor operating point. Moreover, the compressor cannot reach its maximum efficiency since it lies at the surge line.

Active surge control takes a very different approach from surge avoidance. This approach is intended to deal with surge instead of avoiding it. Therefore, the compressor can perform stably even in its unstable operating region. This means that the stable operating area of the compressor is extended and it can now reach its maximum efficiency.

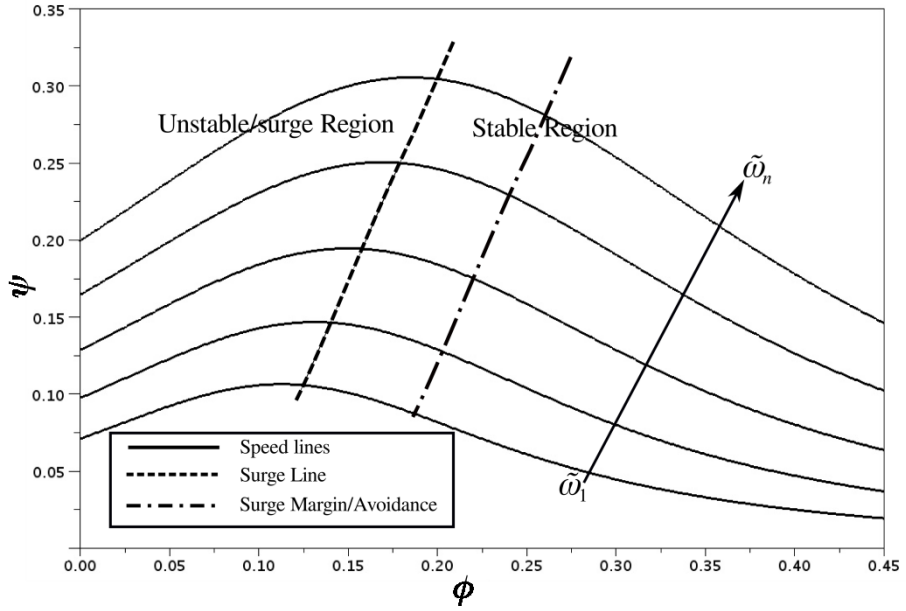

Figure 1 Compressor Map.

Since being introduced by Epstein, *et al*. [1], various aspects of active surge control has been developed. An overview about the development in model, sensor and actuator can be found in [2,3]. Several approaches to approximate

compressor characteristics are tested and discussed in [4]. In the area of control strategies, several methods have been applied, namely proportional-integral control [5], globally stabilizing switching controllers [6], backstepping [7,8], and linear quadratic regulation (LQR) with integral action [9]. It is worth mentioning that the control strategies in [5-10] are applied to a centrifugal compressor model with spool dynamics.

In this study, an equivalent linear form of state and input matrices was obtained by applying nonlinearity cancellation [11] to the model and linearizing the compressor characteristic. As a framework, the Moore-Greitzer compressor model with spool dynamics, developed in [5,6], was used. Throttle and torque were chosen as actuators as in [6]. Any loss occurring in the actuators, such as friction loss, was not taken into consideration. Finally, an LQR plus integrator was chosen as the controller.

2 Model

2.1 Model and Compressor Characteristic

The compression system under study consists of centrifugal compressor, duct, plenum and throttle, as shown in Figure 2. This scheme is related to the Moore-Greitzer model with spool dynamics, which was developed by Gravdahl [5] and nondimensionalized by Leonessa, *et al.* [6] as:

$$\begin{bmatrix} \dot{\psi} \\ \dot{\phi} \\ \dot{\tilde{\omega}} \end{bmatrix} = \begin{bmatrix} 0 & \bar{a} & 0 \\ -\bar{b} & \dfrac{\psi_c(\phi,\tilde{\omega})}{\phi}\bar{b} & 0 \\ 0 & 0 & -|\phi|\sigma\bar{c} \end{bmatrix} \begin{bmatrix} \psi \\ \phi \\ \tilde{\omega} \end{bmatrix} + \begin{bmatrix} -\sqrt{\psi}\bar{a} & 0 \\ 0 & 0 \\ 0 & \bar{c} \end{bmatrix} \begin{bmatrix} \gamma_{th} \\ \tau \end{bmatrix} \tag{1}$$

where ψ is nondimensional pressure ratio, ϕ non-dimensional massflow, $\tilde{\omega}$ nondimensional rotational speed, $\psi_c(\phi, \tilde{\omega})$ is compressor characteristic, $\gamma_{th}\sqrt{\psi}$ and τ are throttle and torque inputs, respectively, while $\dot{(\,)}$ refers to derivation of a state against nondimensional time ξ. The parameters $\bar{a}$, $\bar{b}$ and $\bar{c}$ represent compressor physical quantities, which are defined as [6]:

$$\bar{a} = \frac{L_c^3}{V_p} \tag{2}$$

$$\bar{b} = \frac{L_c^2}{A_1}, \tag{3}$$

and:

$$\bar{c} = \frac{L_c^3 r_2^2 p_{01}}{a_{01}^2 J}, \tag{4}$$

where L_c is duct length, V_p plenum volume, A_1 inducer (impeller eye) area, r_2 radius of impeller tip, p_{01} pressure at inlet, a_{01} sonic velocity at inlet, and J moment of inertia.

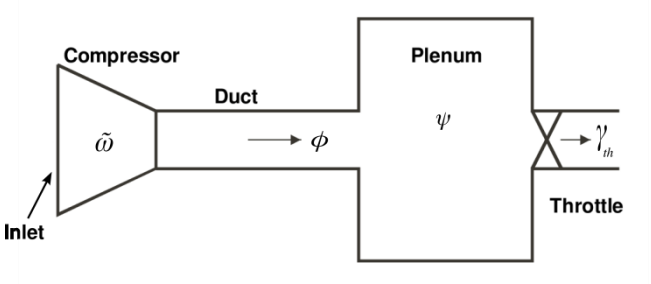

Figure 2 Schematic diagram of compression system [10].

The compressor characteristic is the ratio between the pressures at the compressor's downstream and upstream flow (inlet), denoted in Figure 2 as p_{02} and p_{01}, respectively. Several approaches to approximate compressor characteristics are discussed in [4]. In this paper, a physical-based compressor characteristic is used. This characteristic was derived by Gravdahl [5], experimentally validated by Gravdahl, *et al.* [12], and has been used in [6]. In nondimensional form, it is defined as [6]:

$$\psi_c(\phi,\tilde{\omega}) = \left[1 + \eta_c(\phi,\tilde{\omega})\bar{d}\sigma\tilde{\omega}^2\right]^{\frac{\kappa}{\kappa-1}}, \tag{5}$$

where $\eta_c(\phi, \tilde{\omega})$ is compressor isentropic efficiency, and σ a slip factor between inducer and impeller tip. Parameters κ and $\bar{d}$ are given by [5-6]:

$$\kappa = \frac{c_p}{c_v}, \tag{6}$$

$$\bar{d} = \frac{a_{01}^2}{c_p T_{01}}, \tag{7}$$

where c_p and c_v are specific heat at constant pressure and volume respectively, while T_{01} is inlet temperature.

Isentropic efficiency is defined as [5-6]:

$$\eta_c(\phi, \tilde{\omega}) = \frac{\Delta h_{0c,ideal}}{\Delta h_{0c,ideal} + \Delta h_{loss}}, \tag{8}$$

where $\Delta h_{0c,ideal}$ is specific enthalpy delivered to the fluid without taking account of the losses [5]. In nondimensional form, it is defined as [6]:

$$\Delta h_{0c,ideal} = \sigma \tilde{\omega}^2. \tag{9}$$

On the other hand, Δh_{loss} is the sum of losses in the compression system that is defined as [5]:

$$\Delta h_{loss} = \Delta h_{ii} + \Delta h_{di} + \Delta h_{if} + \Delta h_{df}, \tag{10}$$

where Δh_{ii} and Δh_{di} are incidence losses at the inducer and diffuser respectively, while Δh_{fi} and Δh_{fd} are friction losses at the inducer and diffuser respectively. In nondimensional form, these losses are defined as [6]:

$$\Delta h_{ii} = \frac{1}{2}\left(f_1 \tilde{\omega} - f_2 \phi\right)^2, \tag{11}$$

$$\Delta h_{di} = \frac{1}{2}\left(\sigma \tilde{\omega} - f_3 \phi\right)^2, \tag{12}$$

$$\Delta h_{if} = f_4 \phi^2, \tag{13}$$

and:

$$\Delta h_{df} = f_5 \phi^2, \tag{14}$$

where $f_i, i = 1 \ldots 5$ are nondimensional parameters. To find the details of the dimensional parameters represented by f_i, the reader may consult [5]. In compression system operation, the compressor characteristic as defined in (5) applies for positive massflow. For negative massflow, the compressor characteristic is defined as [6]:

$$\psi_c(\phi,\tilde{\omega}) = \mu\phi^2 + \psi_{c0}\,,\phi < 0\,, \tag{15}$$

where $\mu > 0$ and [6]:

$$\psi_{c0}(\phi\ ,\tilde{\omega}) = \left[\left(1+\eta_{c0}\sigma\bar{d}\tilde{\omega}^2\right)^{\frac{\kappa}{\kappa-1}} - 1\right]_{\phi=0}\,, \tag{16}$$

and [6] :

$$\eta_{c0} = \eta_c(\phi\ ,\tilde{\omega})_{\phi=0} = \frac{2\sigma}{\sigma^2 + 2\sigma + f_1}\,. \tag{17}$$

2.2 Surge Line

The surge line is defined as the line that passes through the maxima of the compressor characteristic [5]. Hence, from $\partial\psi_c(\phi,\tilde{\omega})/\ \partial\phi = 0$, it is found that the surge line for any speed line as described in Figure 1 will pass through the extreme point:

$$\left[\phi_{sl}\quad \psi_{sl}\right] = \left[k_f\tilde{\omega}^2\quad \psi_c(\phi,\tilde{\omega})\ _{\phi=\phi_{sl}}\right]. \tag{18}$$

where index sl refers to the surge line and k_f is a constant that is defined as [6]:

$$k_f = \frac{f_1 f_2 + \sigma f_3}{f_2^2 + f_3^2 + 2f_4 + 2f_5}\,. \tag{19}$$

As implied by (18), the compressor's maximum pressure ratio exists right at the surge point. The compressor's maximum isentropic efficiency is also achieved at this point [6]. However, a small reduction in massflow from this point will lead the compressor into surge.

2.3 Model and Compressor Characteristic Modifications

Both the compressor model (1) and itscharacteristic (5) are highly nonlinear. In order to apply linear control theory to (1), the following approaches are used:

(i) Cancellation of the nonlinear components [11], which exist at states ψ and $\tilde{\omega}$ in (1), by transferring them into the input vectors.

(ii) Linearization of the compressor characteristic (5) around the surge point in the stable region and in the unstable region as well.

By approach (i), states ψ and $\tilde{\omega}$ in (1) appear linear, that is:

$$\begin{bmatrix} \dot{\psi} \\ \dot{\phi} \\ \dot{\tilde{\omega}} \end{bmatrix} = \begin{bmatrix} 0 & \bar{a} & 0 \\ -\bar{b} & \dfrac{\psi_c(\phi,\tilde{\omega})}{\phi}\bar{b} & 0 \\ 0 & 0 & -\bar{c} \end{bmatrix} \begin{bmatrix} \psi \\ \phi \\ \tilde{\omega} \end{bmatrix} + \begin{bmatrix} -\bar{a} & 0 \\ 0 & 0 \\ 0 & \bar{c} \end{bmatrix} \begin{bmatrix} v_1 \\ v_2 \end{bmatrix}, \tag{20}$$

where v_1 and v_2 are newly defined control inputs given by:

$$v_1 = \gamma_{th}\sqrt{\psi}\,, \tag{21}$$

and:

$$v_2 = \tau - \sigma\tilde{\omega}(|\phi| - 1). \tag{22}$$

Approach (ii) is applied based on the fact that surge point (18) is the point where the system is in steady-state condition. In this condition, the following relations apply [6]:

$$[\psi_{ss} \quad \phi_{ss} \quad \tilde{\omega}_{ss}] = [\psi_{css} \quad v_{1ss} \quad v_{2ss}], \tag{23}$$

where index ss refers to the steady-state condition. Inspired by Leonessa, *et al*. [6], linear compressor characteristics are derived by defining a small operating range of each region relative to the steady-state point. For the unstable region, such range is defined by:

$$x_1 = \psi_{ss} - \psi, \tag{24}$$

$$x_2 = \phi_{ss} - \phi, \tag{25}$$

$$x_3 = \tilde{\omega}_{ss} - \tilde{\omega}\,, \tag{26}$$

$$\hat{v}_1 = v_{1ss} - v_1\,, \tag{27}$$

and:

$$\hat{v}_2 = v_{2ss} - v_2\,. \tag{28}$$

Assuming the operating range defined by (24)-(28) is linear, the compressor characteristic can be defined as:

$$\psi_c(x_2, x_3) = \psi_c(\phi_{ss}, \tilde{\omega}_{ss}) - \psi_c(\phi, \tilde{\omega}). \tag{29}$$

Furthermore, linearization (5) near ϕ_{ss} and $\tilde{\omega}_{ss}$ using Taylor expansion results in:

$$\psi_c(\phi,\tilde{\omega}) \approx \psi_c(\phi_{ss},\tilde{\omega}_{ss}) + (\phi-\phi_{ss})\frac{\partial\psi_c(\phi_{ss},\tilde{\omega}_{ss})}{\partial\phi} + (\tilde{\omega}-\tilde{\omega}_{ss})\frac{\partial\psi_c(\phi_{ss},\tilde{\omega}_{ss})}{\partial\tilde{\omega}} \quad . \tag{30}$$

The value of $\psi_c(\phi_{ss},\tilde{\omega}_{ss})$ is obtained by substituting $\phi=\phi_{ss}$ and $\tilde{\omega}=\tilde{\omega}_{ss}$ into (5). On the other hand, substituting $\phi=\phi_{ss}$ and $\tilde{\omega}=\tilde{\omega}_{ss}$ into:

$$\frac{\partial\psi_c(\phi,\tilde{\omega})}{\partial\phi} = \frac{\kappa}{\kappa-1}\left(1+\eta_c(\phi,\tilde{\omega})\sigma\bar{d}\tilde{\omega}^2\right)^{\frac{1}{\kappa-1}} \times\left[\frac{\sigma^2\tilde{\omega}^4(\phi)\left(f_2^2+f_3^2-2f_4-2f_5\right)-\tilde{\omega}(f_1f_2+f_3\sigma)}{\left(\sigma\tilde{\omega}^2+\frac{1}{2}(f_1\tilde{\omega}-f_2\phi)^2+\frac{1}{2}(\sigma\tilde{\omega}-f_3\phi)^2+f_4\phi^2+f_5\phi^2\right)^2}\right], \tag{31}$$

and:

$$\frac{\partial\psi_c(\phi,\tilde{\omega})}{\partial\tilde{\omega}} = \frac{\kappa}{\kappa-1}\left(1+\eta_c(\phi,\tilde{\omega})\sigma\bar{d}\tilde{\omega}^2\right)^{\frac{1}{\kappa-1}} \times\left[\frac{\sigma^2\bar{d}\tilde{\omega}^3\left(k_1\tilde{\omega}^2-k_2\tilde{\omega}+k_2\phi^2\right)}{\left(\sigma\tilde{\omega}^2+\frac{1}{2}(f_1\tilde{\omega}-f_2\phi)^2+\frac{1}{2}(\sigma\tilde{\omega}-f_3\phi)^2+f_4\phi^2+f_5\phi^2\right)^2}\right], \tag{32}$$

results in $\partial\psi_c/\partial\phi(\phi_{ss},\tilde{\omega}_{ss})$ and $\partial\psi_c/\partial\tilde{\omega}(\phi_{ss},\tilde{\omega}_{ss})$, respectively. Substituting (30) into (29) results in the compressor characteristic at the unstable (surge) region, that is:

$$\psi_c(\phi,\tilde{\omega}) = \beta\phi + \gamma\tilde{\omega}, \tag{33}$$

where:

$$\beta = \frac{\partial\psi_c}{\partial\phi}(\phi_{ss},\tilde{\omega}_{ss}), \tag{34}$$

and:

$$\gamma = \frac{\partial\psi_c}{\partial\tilde{\omega}}(\phi_{ss},\tilde{\omega}_{ss}). \tag{35}$$

Remark 1. *According to [5], surge occurs at points with positive slope in the compressor characteristic curve. However, calculation of (30) uses* $\phi < \phi_{ss}$ *, thus* $x_2 < 0$ *. Therefore* $\partial \psi_c(\phi, \tilde{\omega}) / \partial \phi$ *in (31) must be negative, so that (33) has a positive slope.*

Substituting (24)-(28), differentiation of (24)-(26) and (33) into (20) results in a linear compressor model for the surge region:

$$\begin{bmatrix} \dot{\psi} \\ \dot{\phi} \\ \dot{\tilde{\omega}} \end{bmatrix} = \begin{bmatrix} 0 & \bar{a} & 0 \\ -\bar{b} & \alpha\beta\bar{b} & \alpha\gamma\bar{b} \\ 0 & 0 & -\bar{c} \end{bmatrix} \begin{bmatrix} \psi \\ \phi \\ \tilde{\omega} \end{bmatrix} + \begin{bmatrix} -\bar{a} & 0 \\ 0 & 0 \\ 0 & \bar{c} \end{bmatrix} \begin{bmatrix} \hat{v}_1 \\ \hat{v}_2 \end{bmatrix}. \tag{36}$$

Parameter $\alpha > 0$ in (36) is a coefficient that guarantees $\psi_{ss} = \psi_{css}$ in (23) will be achieved, where:

$$\alpha = \frac{\psi_{ss}}{-\beta\phi_{ss} + \gamma\tilde{\omega}_{ss}}. \tag{37}$$

For the stable region, a small operating range relative to the steady-state point is defined by:

$$x_{1r} = \psi - \psi_{ss} \ , \tag{38}$$

$$x_{2r} = \phi - \phi_{ss} \ , \tag{39}$$

$$x_{3r} = \tilde{\omega} - \tilde{\omega}_{ss} \ , \tag{40}$$

$$\hat{v}_{1r} = v_1 - v_{1ss} \ , \tag{41}$$

and:

$$\hat{v}_{2r} = v_2 - v_{2ss} \ . \tag{42}$$

The index r in (38)-(42) refers to the stable region. Assuming the range defined by (38)-(42) is linear, the compressor characteristic for the unstable region can be defined as [6]:

$$\psi_c(x_{2r}, x_{3r}) = \psi_c(\phi_{ss} + x_{2r}, \tilde{\omega}_{ss} + x_{3r}) - \psi_c(\phi_{ss}, \tilde{\omega}_{ss}). \tag{43}$$

Substituting (38)-(40) into (30) and subsequently substituting its result into (43) results in:

$$\psi_c(\phi, \tilde{\omega}) = \beta\phi + \gamma\tilde{\omega} \ . \tag{44}$$

Remark 2. *The difference between (33) and (44) lies in their respective operating regions. In (44),* $\phi > \phi_{ss}$, *thus* $x_{2r} > 0$. *Since* $\partial\psi_c(\phi,\tilde{\omega})/\partial\phi$ *is negative, the slope in (44) will be also negative.*

The linear compressor model for the stable region is obtained by substituting (38)-(42), differentiation of (38)-(40) and (44) into (20), that is:

$$\begin{bmatrix}\dot{\psi}\\ \dot{\phi}\\ \dot{\tilde{\omega}}\end{bmatrix}=\begin{bmatrix}0 & \bar{a} & 0\\ -\bar{b} & \alpha_r\beta\bar{b} & \alpha_r\gamma\bar{b}\\ 0 & 0 & -\bar{c}\end{bmatrix}\begin{bmatrix}\psi\\ \phi\\ \tilde{\omega}\end{bmatrix}+\begin{bmatrix}-\bar{a} & 0\\ 0 & 0\\ 0 & \bar{c}\end{bmatrix}\begin{bmatrix}\hat{v}_{1r}\\ \hat{v}_{2r}\end{bmatrix}. \tag{45}$$

Parameter $\alpha_r > 0$ in (45) is a coefficient that guarantees that $\psi_{ss} = \psi_{css}$ in (23) is achieved, where:

$$\alpha_r = \frac{\psi_{ss}}{\beta\phi_{ss} + \gamma\tilde{\omega}_{ss}}. \tag{46}$$

2.4 Defining Switching Function for Compressor Models

By observation on (36) and (45), it was shown that the general form of these two models is similar. Hence, it is of interest to find a switching function that determines when the system is in stable mode or in unstable mode.

The characteristic equation of the state matrix in (36) *or* (45):

$$\mathbf{A}=\begin{bmatrix}0 & \bar{a} & 0\\ -\bar{b} & \alpha\beta\bar{b} & \alpha\gamma\bar{b}\\ 0 & 0 & -\bar{c}\end{bmatrix}, \tag{47}$$

is given by:

$$(\lambda+\bar{c})(\lambda^2+\alpha\beta\bar{b}\lambda+\bar{a}\bar{b})=0. \tag{48}$$

By inspection of (47) it is found that open-loop stability depends solely on the sign of $\mathbf{A}_{2,2}$, both in (36) and (45). This is because α (or α_r), $\bar{a}$, $\bar{b}$ and $\bar{c}$ are all constant and positive, while β is negative. If $\mathbf{A}_{2,2}$ is positive, $\mathbf{A}$ will be stable, since its eigen values are all negative. Conversely, if $\mathbf{A}_{2,2}$ is negative, $\mathbf{A}$ is unstable, since at least one of its eigen values is positive. These facts are in accordance with the definition of negative and positive slope in (33) and (44).

Hence, a switching function is adequate to define stable and unstable region mode. A switching function is then inserted to $\mathbf{A}_{2,2}$, such that:

$$\mathbf{A}_{2,2} = f_s \alpha \beta \bar{b} , \tag{49}$$

where:

$$f_s = \begin{Bmatrix} -1 & if \quad \phi < \phi_{ss} \\ 1 & else \end{Bmatrix} . \tag{50}$$

Using (50), (37) and (46) can now be stated into a single function, which is:

$$\alpha = \frac{\psi_{ss}}{f_s \beta_{ss} + \gamma \tilde{\omega}_{ss}} . \tag{51}$$

3 Controller Design

Based on (23), (50) and (51), the control strategy is formulated as follows:

(i) open-loop control is employed from initial condition to surge line

(ii) closed-loop control is employed from surge line to unstable operating point

3.1 Filtering the Control Action

In closed-loop control, the nonlinear component that originally exists in the third-state of (1) will re-appear. However, as indicated in (22), its presence will produce a large additional load for the controller to handle. Such a situation will be disadvantageous for system performance, especially when the control load changes abruptly. To anticipate such problems, a linear low-pass filter with the following impulse response:

$$f_{lpf} = K_{lpf} e^{-t/T} , \tag{52}$$

is introduced to filter v_2 (22). The filter will keep changes in v_2 within a small range. Gain K_{lpf} is set such that the maximum value produced by nonlinearity of v_2 can be moderated, while constant T is set to expedite dissipation of the nonlinearity as time t goes to infinity.

Hence, the closed-loop control inputs in the unstable region are obtained by incorporating (21) and (27):

$$\gamma_{th} = \frac{v_{1ss} - \hat{v}_1}{\sqrt{\psi}}, \tag{53}$$

and by incorporating (22), (28) and (52):

$$\tau = v_{2ss} - \hat{v}_2 + f_{lpf}\sigma\tilde{\omega}(|\phi| - 1). \tag{54}$$

3.2 LQR plus Integrators Design

From the general form of state space equations:

$$\dot{\mathbf{x}} = \mathbf{A}\mathbf{x} + \mathbf{B}\hat{\mathbf{v}} + \mathbf{G}\mathbf{w}, \tag{55}$$

$$\mathbf{y} = \mathbf{C}\mathbf{x} + \mathbf{D}\hat{\mathbf{v}}, \tag{56}$$

with all the outputs assumed to be measurable. In order to incorporate error, an augmented state is introduced [13]:

$$\begin{bmatrix} \dot{\mathbf{x}} \\ \dot{\mathbf{e}} \end{bmatrix} = \begin{bmatrix} \mathbf{A}\mathbf{x} + \mathbf{B}\mathbf{v} \\ \mathbf{y}_{ref} - \mathbf{C}\mathbf{x} \end{bmatrix}, \tag{57}$$

where $\mathbf{e}$ and $\mathbf{y}_{ref}$ are the output error and set point vectors, respectively. In the form of (55), (57) can be written as:

$$\dot{\tilde{\mathbf{x}}} = \tilde{\mathbf{A}}\tilde{\mathbf{x}} + \tilde{\mathbf{B}}\tilde{\mathbf{v}} + \tilde{\mathbf{y}}_{ref}, \tag{58}$$

where:

$$\tilde{\mathbf{A}} = \begin{bmatrix} \mathbf{A} & \mathbf{0} \\ \mathbf{0} & \mathbf{0} \end{bmatrix}, \tag{59}$$

$$\tilde{\mathbf{B}} = \begin{bmatrix} \mathbf{B} & \mathbf{0} \end{bmatrix}^T, \tag{60}$$

$$\tilde{\mathbf{y}}_{ref} = \begin{bmatrix} \mathbf{y}_{ref} & \mathbf{0} \end{bmatrix}^T. \tag{61}$$

Furthermore, the standard quadratic performance index form of (58) is written as [14]:

$$J = \frac{1}{2}\int_0^\infty \left[\tilde{\mathbf{x}}^T\tilde{\mathbf{Q}}\tilde{\mathbf{x}} + \tilde{\hat{\mathbf{v}}}^T\mathbf{R}\tilde{\hat{\mathbf{v}}}\right], \tag{62}$$

where $\tilde{\mathbf{Q}}$ and $\mathbf{R}$ are positive semi-definite and positive definite matrices, respectively. Control signal $\tilde{\hat{\mathbf{v}}}$ is given by:

$$\tilde{\hat{\mathbf{v}}} = \tilde{\mathbf{K}}\tilde{\mathbf{x}}, \tag{63}$$

and:

$$\tilde{\mathbf{K}} = \mathbf{R}^{-1}\tilde{\mathbf{B}}^T\mathbf{P}, \tag{64}$$

where P is a solution of the following Riccati equation [13]:

$$\mathbf{P}\tilde{\mathbf{A}} + \tilde{\mathbf{A}}^T\mathbf{P} - \mathbf{P}\tilde{\mathbf{B}}\mathbf{R}^{-1}\tilde{\mathbf{B}}^T\mathbf{P} + \tilde{\mathbf{Q}} = \mathbf{0}, \tag{65}$$

with:

$$\tilde{\mathbf{Q}} = \begin{bmatrix} \mathbf{C}^T\mathbf{Q}_y\mathbf{C} & \mathbf{0} \\ \mathbf{0} & \mathbf{Q}_e \end{bmatrix}. \tag{66}$$

$\tilde{\mathbf{Q}}$ in (66) is the weighting matrix of $\mathbf{e}$. Substituting the result of (65) in (64), the control gains are obtained:

$$\tilde{\mathbf{K}} = \begin{bmatrix} \mathbf{K}_{sfb} & \mathbf{K}_{\mathbf{e}} \end{bmatrix}, \tag{67}$$

where $\mathbf{K}_{sfb}$ and $\mathbf{K}_{int}$ are state feedback control gain and integrator gain, respectively. Recall that $\tilde{\mathbf{A}}$ and $\tilde{\mathbf{B}}$ are 6×6 and 6×2 matrices, respectively, then $\tilde{\mathbf{K}}$ is a 2×6 matrix. In this case, $\mathbf{K}_{sfb}$ exist at the 1st-3rd column of $\tilde{\mathbf{K}}$, whereas $\mathbf{K}_e$ exists the 4th -6thcolumn. The closed-loop control signal is therefore defined as:

$$\hat{\mathbf{v}} = -\mathbf{K}_{sfb}\mathbf{x} - \mathbf{K}_{\mathbf{e}}\mathbf{e} + \mathbf{K}_{ref}\mathbf{x}_{ref}, \tag{68}$$

where $\mathbf{K}_{ref}$ is reference gain.

4 Simulation

The numerical values used in this simulation were taken from [6]. The Riccati equation in (65) was solved using the built-in Riccati function of Scilab 5.3.2. It was chosen that $\mathbf{R}$ =0.05 and $\tilde{\mathbf{Q}} = diag(5,10.5,10,0.5,0.5)$. It was obtained that:

$$\mathbf{K}_{sfb} = \begin{bmatrix} 32.618 & -16.199 & -14.148 \\ 10.524 & -7.443 & 15.790 \end{bmatrix}, \tag{69}$$

and:

$$\mathbf{K}_e = \begin{bmatrix} 0 & -2.565 & -2.602 \\ 0 & 2.623 & 8.266 \end{bmatrix}. \tag{70}$$

For the linear low-pass filter defined in (52), the numerical values $K_{lpf} = 0.05$ and $T = 5$ were chosen. The simulation was carried out using Scilab 5.3.2 and the 4th Order Runge-Kutta was used as the numerical method.

From initial condition ψ_0 =0.188, ϕ_0 =0.141, $\tilde{\omega}_0$ =0.397, the compressor was brought to steady-state condition ψ_{ss} =0.305, ϕ_{ss} =0.186, $\tilde{\omega}$ =0.493. Using the dimensional values in [5], the steady-state nondimensional values represent ambient pressure p =1.3×10^5 Pa, massflow m =2.19 kg/s and rotating speed ω = 25000 rpm, respectively. The compressor characteristic for the stable region in such point is given by:

$$\psi_{cr}(\phi, \tilde{\omega}) = -0.1565\phi + 0.6787\tilde{\omega}, \tag{71}$$

while the surge region is defined by:

$$\psi_c(\phi, \tilde{\omega}) = 0.1315\phi + 0.5705\tilde{\omega}. \tag{72}$$

At nondimensional time ξ = 0.75, massflow was reduced to ϕ = 0.176, which is 5.38 percent less than the allowed minimum value for $\tilde{\omega}$ =0.493. This means the compressor enters its unstable operating region. Several indicators of the compressor's behavior are represented in Figures 3-7. System response without the closed-loop control is represented by a dotted line, while its counterpart is represented by a solid line.

As shown in Figures 3-4, the modified model and characteristic can describe the surge behavior. On the other hand, the closed-loop control managed to keep the compressor stable when being operated in the unstable region.

It should be noted that massflow is actually difficult to measure [15]. Hence, incorporating a massflow observer as proposed in [15] to the model could give more realistic results.

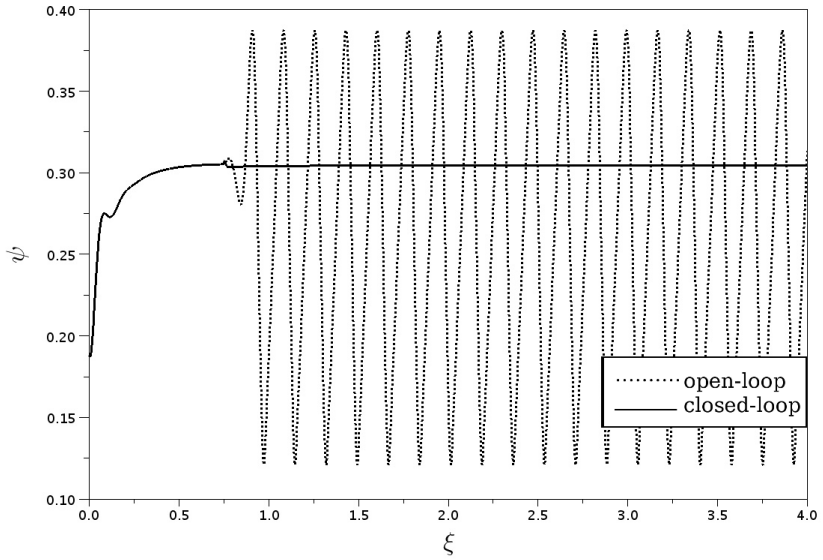

Figure 3 Pressure ratio against nondimensional time.

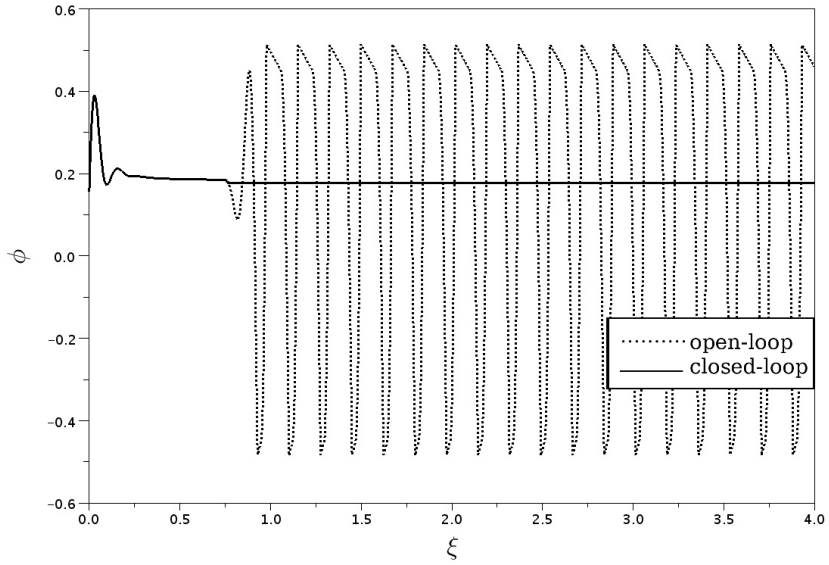

Figure 4 Massflow against nondimensional time.

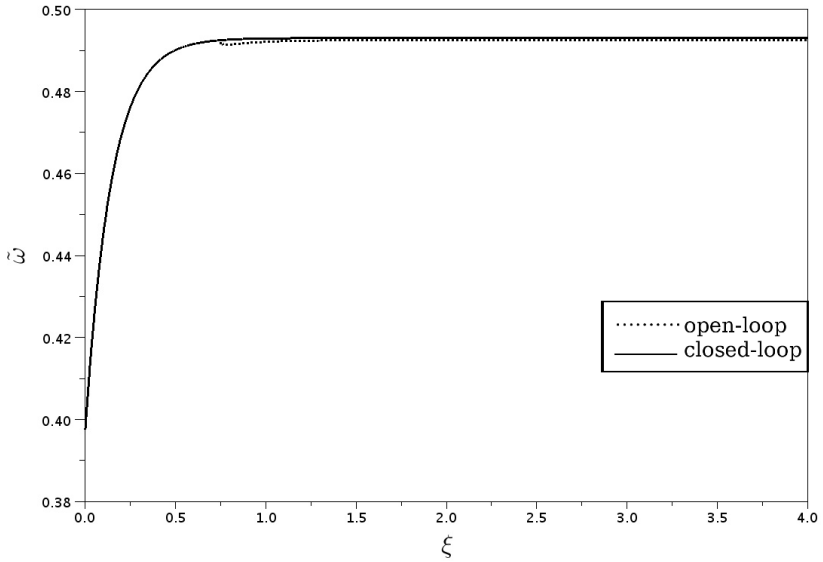

Figure 5 Rotating speed against nondimensional time.

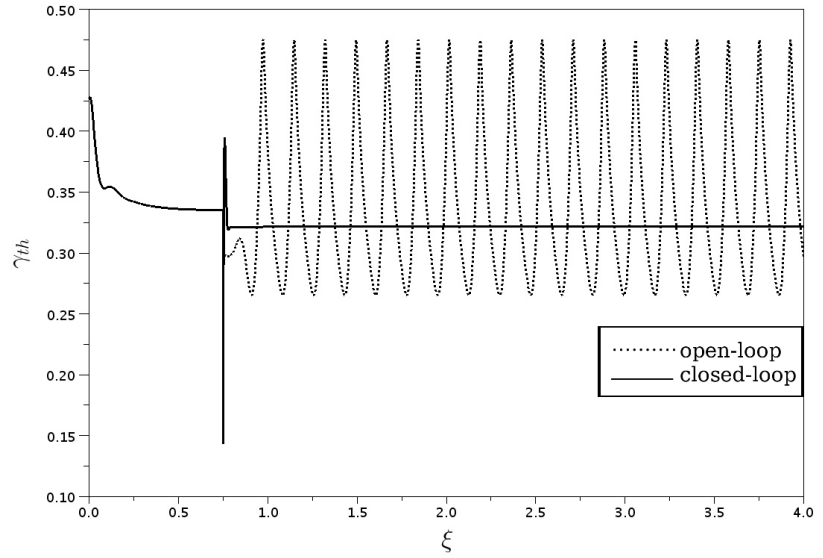

Figure 6 Throttle opening against nondimensional time.

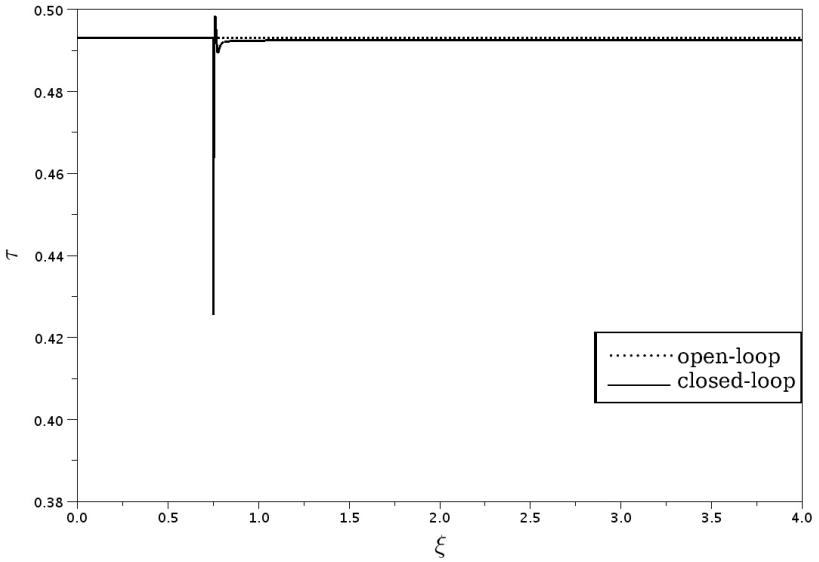

Figure 7 Torque against nondimensional time.

5 Conclusion

An active control of centrifugal compressors via model nonlinear component cancellation and characteristics linearization has been presented. By simulation it was shown that the modified model and characteristic can describe the surge behavior. The closed-loop controller managed to keep the compressor stable when operated in the unstable region.

Inherently, linear realization of the active surge of compression systems has limitations within the range of the unstable operating region as to what it can cope with. However, the simpler design and analysis used can be seen as a trade-off for its nonlinear counterpart. On the other hand, its achievement in dealing with surge is still a departure from the surge avoidance approach.

References

[1] Epstein, A.H., Ffowcs Williams, J. & Greitzer, E.M., *Active Suppression of Aerodynamic Instabilities in Turbomachines*, Journal of Propulsion and Power, **5**(2), pp. 204-211, 1989.

[2] Gravdahl, J.T. & Egeland, O., *A Moore-Greitzer Axial Compressor Model with Spool Dynamics*, Proc. of the 36th IEEE Conference on Decision and Control, San Diego, CA, 1997.

[3] Willems, F., *Modeling and Bounded Feedback Stabilization of Centrifugal Compressor Surge*, PhD Thesis, Technische Universiteit Eindhoven, Eindhoven, Netherlands, 2000.
[4] Grong, T.S., *Modeling of Compressor Characteristics and Active Surge Control*, MS Thesis, Norwegian University of Science and Technology, Trondheim, Norway, 2009.
[5] Gravdahl, J.T., *Modeling and Control in Centrifugal Compressor*, PhD thesis, Norwegian University of Science and Technology, Trondheim, Norway, 1998.
[6] Leonessa, A., Haddad, W.M. & Li, H., *Globally Stabilizing Switching Controllers for A Centrifugal Compressor Model with Spool Dynamics*, IEEE Trans. Control Systems Technology, **8**(3), pp. 474-482, 2000.
[7] Bøhagen, B. & Gravdahl, J.T., *Active Surge Control of Compression System Using Drive Torque: A Backstepping Approach*, In: Proc. of the 44th IEEE Conference on Decision and Control, Seville, Spain, 2005.
[8] Bøhagen, B. & Gravdahl, J.T., *Active Surge Control of Compression System Using Drive Torque,* Automatica, **44**(4), pp.1135-1140,2008.
[9] Uddin, N. & Gravdahl, J.T., *Piston-Actuated Active Surge Control of Centrifugal Compressor Including Integral Action*, In: Proc. of the 11th International Conference on Control, Automation and Systems, Gyeonggi-do, Korea, 2011.
[10] Gravdahl, J.T., Egeland, O. & Vatland, S.O., *Drive Torque Actuation in Active Surge Control of Centrifugal Compressors*, Automatica, **38** (2002), pp.1881-1893, 2002.
[11] Khalil, H., *Nonlinear Systems,* Third Edition, Prentice-Hall, Upper-Saddle River, NJ, 2002.
[12] Gravdahl, J.T., Willems, F., De Jager, B. & Egeland, O., *Modeling for Surge Control of Centrifugal Compressors: Comparison with Experiment*, In: Proc. of the 39th IEEE Conference on Decision and Control, Sidney, Australia, 2000.
[13] Åstrom, K.J. & Murray, R.M., *Feedback Systems: An Introduction for Scientists and Engineers*, Princeton University Press, Princeton, NJ, 2008.
[14] Naidu, D.S., *Optimal Control Systems*, CRC Press, Boca Raton, FL, 2003.
[15] Bøhagen, B. & Gravdahl, J.T., *On Active Surge Control of Compressors Using A Mass Flow Observe*r, In: Proc. of the 41st IEEE Conference on Decision and Control, Las Vegas, NV, 2002.